



## Characterization of the Shear Response of Unidirectional Non-Crimp Carbon Fiber Fabrics

A. Trejo<sup>1</sup>, M. Ghazimoradi<sup>1</sup>, C. Butcher<sup>2</sup> and J. Montesano<sup>1</sup> \*

<sup>1</sup> Composites Research Group, Department of Mechanical and Mechatronics Engineering, University of Waterloo, Waterloo, Canada

<sup>2</sup> Department of Mechanical and Mechatronics Engineering, University of Waterloo, Waterloo, Canada

\* Corresponding author (john.montesano@uwaterloo.ca)

### ABSTRACT

Structural carbon fiber/epoxy composite parts comprised of a heavy-tow (50K filaments/tow) Unidirectional Non-crimp Fabric (UD-NCF) and fabricated by high-pressure resin transfer molding (HP-RTM) are a cost-effective option for lightweighting of high-volume production vehicles. The fabric preforming step preceding resin infiltration for HP-RTM processes can promote shear induced fabric wrinkling, which is specific to part geometry and influenced by the selected processing parameters, mold features and fabric architecture. Thus, there is a need to study the shear response and associated local deformation mechanisms of dry UD-NCFs to better inform fabric draping simulation models used to predict defects. In this study a dry carbon fiber UD-NCF was characterized using both picture frame and off-axis extension tests. The study showed the relation between the local deformation and state of the stitching web and the bulk deformation response of the fabric. Also, when subjecting the fabric to shear deformation, a strong correlation between the emergence of defects, such as tow gapping and micro-buckling, was reported. The generated data can be used to calibrate fabric draping models to improve the predictability of defects during draping and ultimately the mechanical performance of the as-manufactured composite part.

**KEYWORDS:** unidirectional non-crimp fabric (UD-NCF), dry fabric characterization, shear response

### 1 INTRODUCTION

Improving energy consumption efficiency in vehicles is of utmost importance to curb CO<sub>2</sub> emissions. Structural lightweighting is perhaps the most effective way to improve vehicle fuel economy and extend the range of battery-electric vehicles. To this end, carbon fiber reinforced epoxy composites have been identified as key automotive materials due to their high specific strength/stiffness, anisotropic tailorability and excellent fatigue performance characteristics [1]. To facilitate the design and certification of composite structural parts, accurate and reliable computational models must be developed to predict their performance. Localized manufacturing defects, which can notably impact the performance of composite parts, can be accounted for by computational models to increase the fidelity of predicting complex deformation and failure modes. These defects can be predicted through process simulation models [2], [3].

Heavy-tow (50K filaments/tow) Unidirectional Non-crimp Fabric (UD-NCF) epoxy-based composite materials fabricated by high-pressure resin transfer molding (HP-RTM) represent a cost-effective option for lightweighting of high-volume production vehicles. Fabric preforming or draping is a key step that precedes resin infiltration in HP-RTM processes. The presence of defects such as shear induced wrinkling and fiber misalignment may reduce the local mechanical properties of the composite part. As such, for HP-RTM parts it is important to predict fiber orientation and the introduction of defects during the draping process, which requires characterization of the specific dry fabric.

In fabrics, the formation of defects is influenced by the combination of bending [4], tensile and shear stiffness properties which have been widely characterized for balanced fabrics [5]–[10]. These properties are challenging to measure in unbalanced fabrics and have been scarcely studied for UD-NCF [11]. This study focused on obtaining the shear response of a UD-NCF. Two common tests are employed, the Picture Frame Test (PFT) and Bias-extension Test. The interpretation of the latter needs to be adapted for UD-NCF due to the asymmetric response; thus, it is referred to as the off-axis extension test (OET) hereafter.

## 2 MATERIAL

The UD-NCF fabric characterized in this study is the heavy tow PX35-UD300 (Zoltek), shown in Figure 1. The fabric consists of 5 mm wide tows, each containing 50K carbon fiber filaments. The tows extend parallel to each other in a single direction and are stitched together with a polyester thread using a tricot pattern. For structural support, glass fibers run perpendicular to the carbon fiber tows, resting between the tows and the polyester stitching. The glass fibers and the stitching have a linear density of 34 and 76 dtex respectively, while the carbon fiber tows have a linear density of 37,400 dtex. The fabric also comprised of a thermosetting binder to allow for preforming. The total areal density of the fabric is 333 g/m<sup>2</sup> with the carbon fibers accounting for over 92% of the total weight.

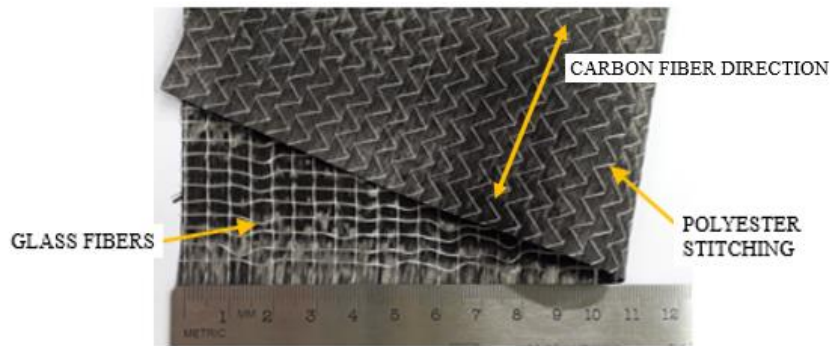


Figure 1: Unidirectional carbon fiber fabric, Zoltek PX35 UD-300.

## 3 EXPERIMENTAL SETUP AND TEST PROCEDURE

The PFT and two OET's, with the fabric biased at 45° and 60° with respect to the loading axis, were conducted to measure the shear response of the fabric. A random speckle pattern was applied to the surface of the specimen and the Digital Image Correlation (DIC) software VIC2D was used to capture deformations during the 45° OET. A clear and well-defined speckle pattern was achieved using white oil based paint applied with a splattering technique. The DIC images were recorded using a Nikon D3200 camera fitted with a Nikon DX Zoom-NIKKOR 28-55 MM lens. The analysis of the DIC images, which had a typical resolution of 0.2646 mm/pixel, was conducted using a Gaussian weights method with a subset size of 55 x 55 square pixels and a step size of 5 pixels. Surface strains were calculated invoking the Green-Lagrange strain tensor and employing a decay filter with size 17. All tests were conducted on a MTS FlexTest SE servo-hydraulic test frame at a displacement rate of 1 mm/s. The applied force was measured by an external load cell with 2.2 kN capacity. This section outlines details of the conducted tests.

### 3.1 Picture Frame Test

The quasi-static picture frame test performed in this study subjected the single layer dry fabric specimen to pure shear deformation using a custom picture frame fixture as seen in Figure 2. With the frame squared, the specimen was clamped with the carbon fiber (CF) tow direction parallel to the frame. The clamping mechanism was designed to prevent the carbon and glass fibers from sliding during loading.

Based on the assumption of uniform deformation, and equating the mechanical work introduced by the frame to the shear deformation energy, the fabric deformation can be described from the crosshead displacement [12]. The change in the shear angle is calculated from the frame arm length ( $L_f$ ) and displacement ( $d_f$ ) according to equation 1.

$$\gamma = 90^\circ - \theta = 90^\circ - 2 \times \cos^{-1} \left( \frac{\sqrt{2} \times L_f + d_f}{2 \times L_f} \right) \quad (1)$$

The shear force is calculated by

$$F_S = \frac{F_f}{2 \cos\left(\frac{\theta}{2}\right)} \quad (2)$$

A normalized force is calculated according to equation 3, where  $L_{\text{fabric}}$  is the side length of the fabric (170 mm) and  $L_{\text{frame}}$  is the side length of the fixture frame (210 mm). It is based on an energy method originally proposed by Peng et al. and adopted in the literature for the characterization of textiles [11], [13].

$$F_N = F_S \frac{L_f}{L_{\text{fabric}}^2} \quad (3)$$

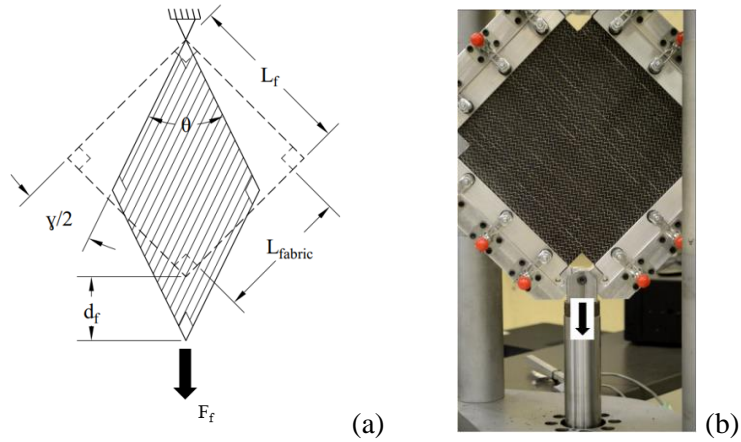


Figure 2: (a) Schematic representation of the deformation induced by the picture frame test (PFT).  
(b) PFT initial position.

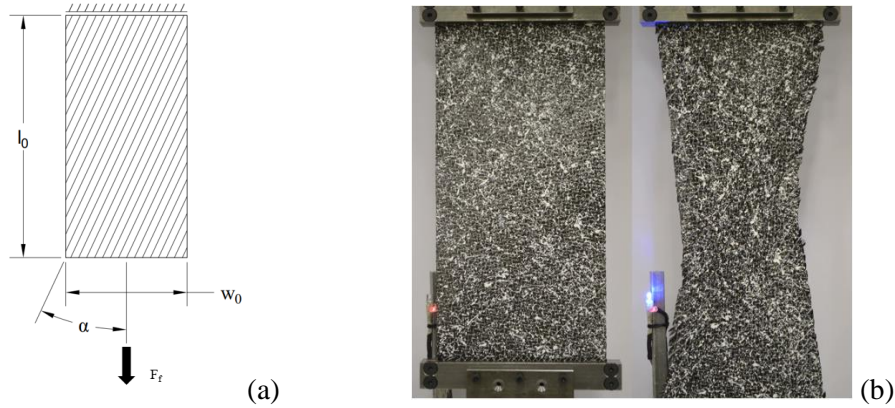


Figure 3: Schematic of the OET (a) and test specimen before and after deformation.

### 3.2 Off-axis Extension Test

Similar to a tensile test, in the OET the sample was pulled with the fibers aligned at an angle from the loading direction,  $45^\circ$  and  $60^\circ$  in this study. The  $45^\circ$  OET was originally developed to measure the trellising behavior of woven fabrics [12]. However, due to the unbalanced nature of UD-NCF, the test assumptions are not applicable, and the results must be analyzed differently than the traditional bias-extension test. The OET is useful to better understand the behavior of the fabric under different loading directions. As presented in Figure 3, the rectangular specimen in the OET is 160 mm wide ( $w_0$ ), 320 mm long ( $l_0$ ) and the angle,  $\alpha$ , represents the direction of the fibers with respect to the loading direction. For these tests, custom grips were used to hold the fabric and the same test frame as the PFT was used to load the specimens in quasi-static tension (1 mm/s).

## 4 TEST RESULTS

### 4.1 Picture Frame Test (PFT)

The PFT load response introduced in Figure 4 **Error! Reference source not found.** represents the average curve from 3 tested specimens, with the error bars representing the corresponding sample standard deviation. A large slope can be observed at the beginning of the curve reaching a maximum normalized force at around  $17^\circ$ . Between shear angles of  $17^\circ$  and  $37^\circ$  the curve has a subtle negative slope before the load response starts increasing again. There are several factors influencing the pure shear response of the fabric. When the fabric is relaxed, the transverse glass fibers are loose, forming kinks in some places as the fabric is handled. In contrast to the glass fibers, the polyester stitching forms a continuous web that is typically free of slack explaining the steep initial shear stiffness. The fabric specimen is clamped with the tows parallel to the sides of the PFT fixtures at the start of the test. This leads to sections of the tricot stitching pattern to cross the CF tows at an angle of approximately  $45^\circ$  from the longitudinal direction, as seen in Figure 5. These stitching sections are put in tension and compression during pure shear deformation as shown in Figure 5. It was observed that the stitching thread sections subjected to tension were responsible for the initial resistance to shear deformation, up to a shear angle of around  $7^\circ$ , at which point they started sliding over the CF tows, eventually inducing meso-buckling in the CF tows. The onset of sliding significantly decreased the shear stiffness before it reaches a zero value at an angle of  $17^\circ$  and a normalized force of 0.127 N/mm. Between the shear angles of  $17^\circ$  and  $37^\circ$ , stitching sliding and carbon fiber tow micro-buckling accommodated the deformation, gradually dropping the normalized force response to 0.120 N/mm. After  $37^\circ$ , a combination of tow compression and, stitching and glass fiber

tensioning caused the load to increase to a global maximum, 0.13 N/mm, at the maximum tested shear angle of 58°.

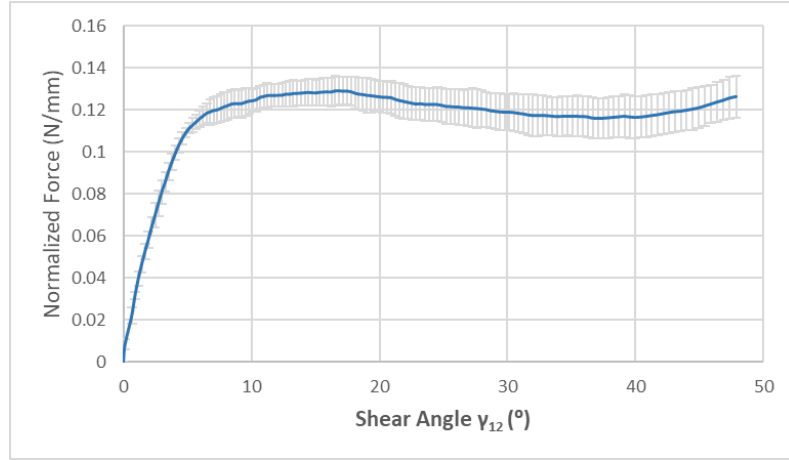


Figure 4: Picture frame test load response versus shear angle.

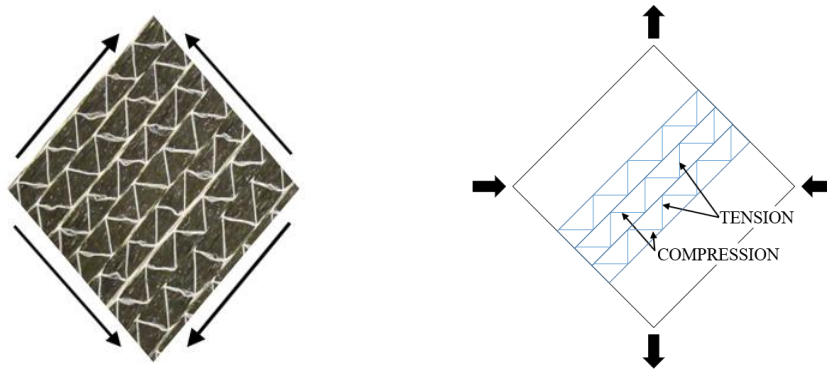


Figure 5: Compression and tensile forces acting on the stitching during the pure shear deformation induced by the picture frame test.

#### 4.2 Off-axis extension test (OET)

OETs at angles of 45° and 60° are compared as these angles were observed to induce in-plane shear and tensile deformation coupling. The curves shown in Figure 6 represent the average curve of three tests and the error bars the corresponding sample standard deviation. The resistance force is similar for both orientations and increases rapidly at the beginning of the test. Then, the slope decreases for both orientations, with the 60° diverging above the 45° curve.

It is observed that at the beginning of the test the interaction between the stitching and the carbon fiber tows tends to resist deformation, rapidly increasing the load response at a rate of 1.67 N/mm. After approximately a 10 mm displacement, stitching-CF tow sliding initiates decreasing the stiffness to approximately 0.30 N/mm. After a 10 mm displacement, the load increases more rapidly in the 60° specimen than the 45° specimen. This shows that the stitching web is stiffer under transverse tensile loading than in shear loading. Assessment of the surface of the 45° specimen under the microscope, after a 10 mm of crosshead displacement, revealed signs of fabric defects such as micro-scale buckling and tow gaping, as seen in Figure 7. The generation of these defects in the fabric seem to be associated with the stiffness degradation after 10 mm displacement as observed in Figure 6.

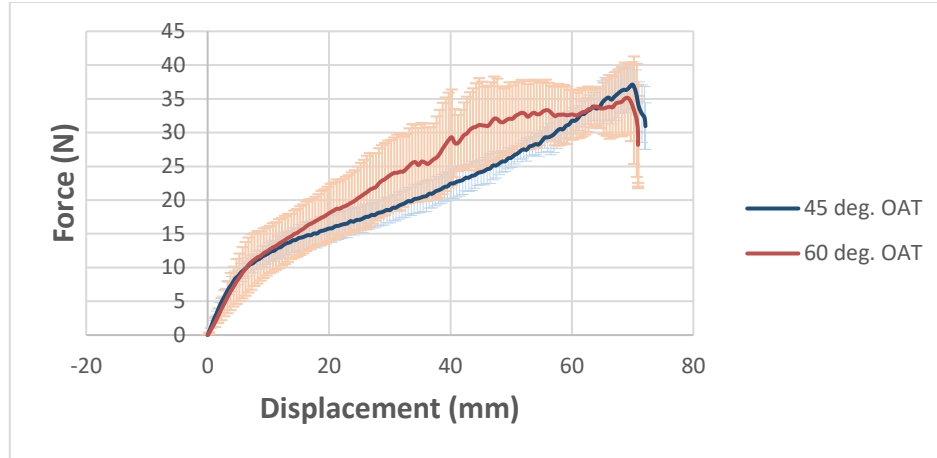


Figure 6: Load response of the 45° and 60° off-axis extension tests.

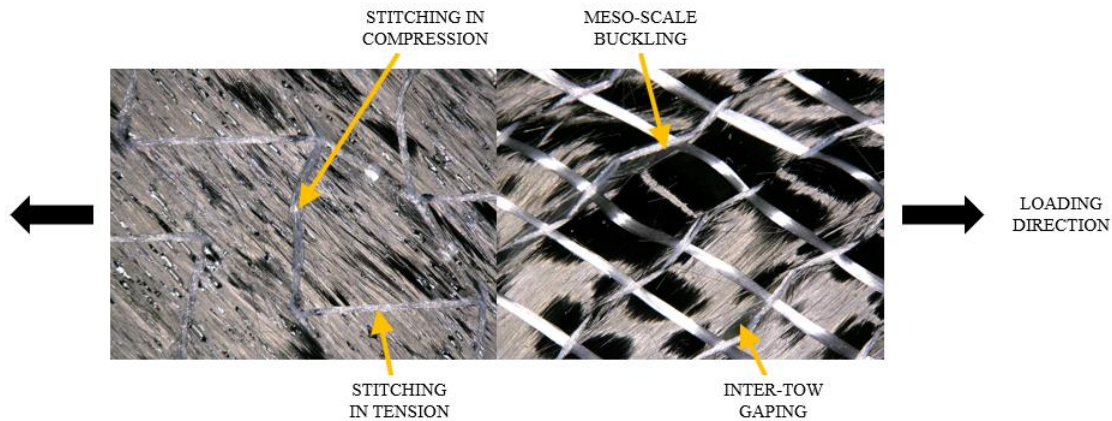


Figure 7: Stitching tension and compression forces causing defects in the fabric at a crosshead displacement of 10 mm during the 45° off-axis extension test.

In order to better characterize the deformation of the 45° OET specimens and understand the interaction between tensile and shear deformation, strain maps of the deformed specimen were captured. Figure 8 presents the in-plane deformation of the fabric when pulled at 45° off-axis angle. Images of the Green-Lagrange strain field at 5 mm, 15 mm and 45 mm were taken as examples of small, medium and large deformation before stitching failure. As expected, the deformation distribution is not uniform along the specimen length. The high stiffness of the locally clamped carbon fibers limits the top and bottom regions of the specimen from deforming, concentrating the deformations in the middle diagonal of the specimen. As seen in Figure 8, the vertical strain,  $xx$ ; the horizontal strain,  $yy$ ; and the shear strain,  $xy$  reach maximum values in the diagonal area along the direction of the carbon fibers.

At large strain, 45 mm displacement, the tensile strain in the load direction,  $xx$ -strain, reached a maximum value of approximately 40%. In the horizontal direction,  $yy$ -strain, there is a maximum compressive strain around the center diagonal of 13% at 15 mm, and 35% at 45 mm. Also, while the tensile strain in the direction of loading is concentrated in the middle of the specimen, high values of shear strain show up close to the free edges of the specimen. Also, along the free edges the perpendicular strain becomes positive as the stitching shifts inward from the vertical edges to accommodate the extension of the specimen. This concentration of tensile, compressive and shear strains along the center diagonal area, where deformation is dominated by the stitching web, indicates a strong influence of the stitching on the in-plane deformation of the fabric.

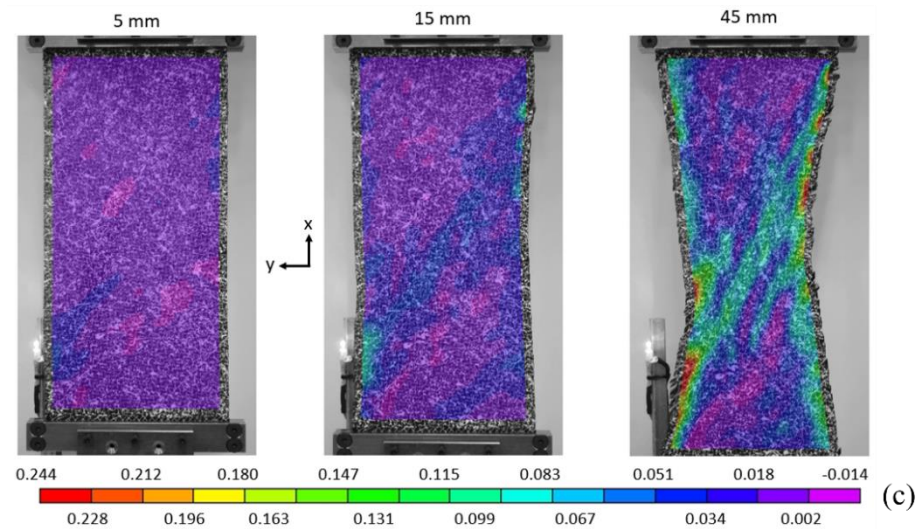
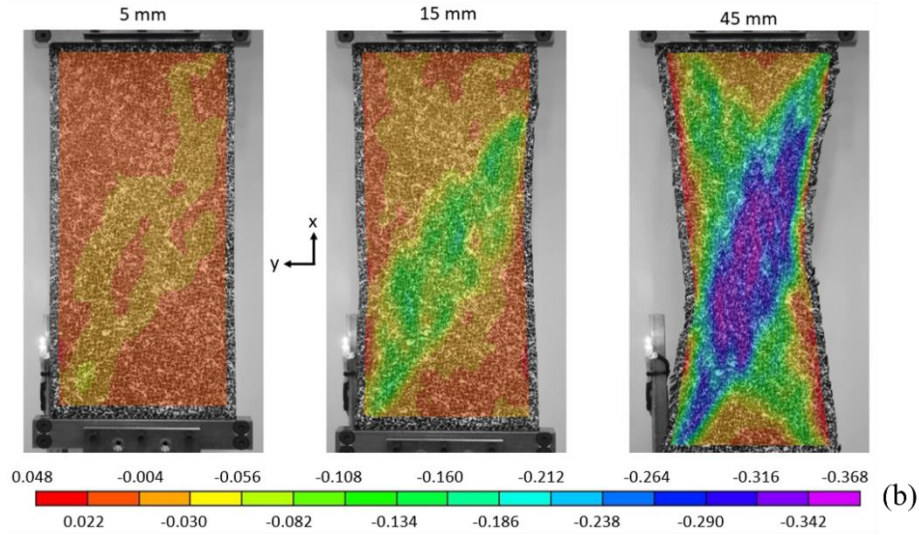
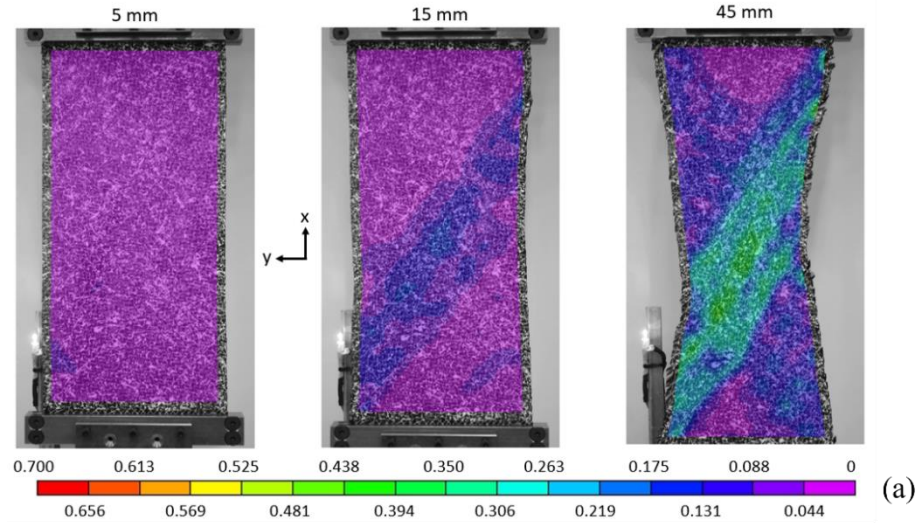


Figure 8: Strain contours for  $45^\circ$  OET captured at indicated displacements, including strain  $xx$  (a), strain  $yy$  (b) and strain  $xy$  (c).

## 5 DISCUSSION

The OET and PFT revealed important deformation patterns in UD-NCF. The PFT is simple to perform, and the results were reasonably repeatable. Additionally, fabric deformation during the PFT was uniform across the sample surface, allowing the kinematics of the material deformation to be readily calculated. A major advantage of the test is that the shear angle can be directly calculated from the crosshead displacement. For the PFT, the stitching was found to be the major factor in the in-plane shear response of the fabric. In particular the behavior of the stitching threads that are aligned in the direction of the shear force and are subjected to tensile forces play a critical role in the in-plane shear response. After a threshold value of shear deformation and once the tow gaps have been closed, these threads start to slide relative to the CF tows causing the fabric shear resistance to stabilize. This constant shear force is observed from 17° to 37° shear angle. Shearing of the fabric revealed that tensioning and compressing of the threads correspondingly parallel and perpendicular to the loading direction are main factors responsible for the shear response of the fabric.

Since the fabric relies on the polyester stitch web and glass fibers for support in the transverse direction, it is expected that during the OET the shear deformation is going to be prevalent in the direction perpendicular to the CF tows. Furthermore, the areas where the stitching is discontinued, such as the two vertical edges in the OET, tend to exhibit larger deformations than the rest of the specimen. Along the free-edge areas, the strain perpendicular to the loading direction changes sign with respect to the compressive strain observed in the middle diagonal. Also, due to the edge-effects, the largest shear strains are seen along the edges. Contrary to the PFT, the deformation distribution induced by the bias extension test is non-uniform across the sample and was calculated through DIC. The OET was useful in assessing the important intra-fabric slipping mechanisms present in UD-NCF. Examination of the OET deformed samples revealed that carbon fiber tow-stitching slip is the most relevant deformation mechanism when the fabric is tensioned at a biased angle from the longitudinal direction. Other observed deformation modes are inter-tow sliding and stitching degradation. A magnified image of the 45° OET at a displacement of approximately 10 mm revealed the formation of defects such as meso-scale buckling and inter-tow gaping.

## 6 CONCLUSIONS

This paper presented observations of an investigation into the shear response of a unidirectional non-crimp fabric (UD-NCF). The in-plane shear response of the non-crimp fabric was obtained at quasi-static loading conditions through the picture frame test (PFT). It was shown that the PFT is an appropriate test to measure the shear resistance of the fabric as it satisfies the uniform shear deformation condition necessary for the validity of the test. Tension and compression were observed in different sections of the stitching thread, which along with inter carbon fiber tow and stitching-tow sliding, were identified as the main interactions responsible for the shear response of the fabric.

Additionally, the shear-tension deformation interaction in the fabric was investigated using an extension tensile test where the fabric is oriented at an angle biased from the load direction, referred to in this paper as the off-axis extension test (OET). The OET induced local shear and compressive strains in the fabric resulting from the global tensile deformation, within the diagonal region along the direction of the carbon fiber tows. A correlation between the emergence of defects and stiffness degradation of the fabric was evidenced in the 320 mm long 45° OET specimen at a displacement of 10 mm. Finally, it was shown that under off-axis tensile loading inter-tow sliding, tow-stitching sliding and stitching degradation are responsible for the deformation kinematics of the fabric.

The quantitative and qualitative data generated in this study can be used to support the development of a material model to numerically simulate the forming process of UD-NCF.

## ACKNOWLEDGEMENTS

The authors would like to thank the Natural Sciences and Engineering Research Council of Canada (NSERC) for their financial support, as well as sponsors Honda R&D Americas, Hexion Inc., Zoltek Corp. and LAVAL International.

## REFERENCES

- [1] T. He, L. Liu, A. Makeev, and B. Shonkwiler, “Characterization of stress–strain behavior of composites using digital image correlation and finite element analysis,” *Compos. Struct.*, vol. 140, pp. 84–93, Apr. 2016.
- [2] T. Gereke, O. Döbrich, M. Hübner, and C. Cherif, “Experimental and computational composite textile reinforcement forming: A review,” *Compos. Part A Appl. Sci. Manuf.*, vol. 46, pp. 1–10, Mar. 2013.
- [3] R. S. Pierce, B. G. Falzon, and M. C. Thompson, “Combining draping and infusion models into a complete process model for complex composite structures COMPLETE PROCESS MODEL FOR MANUFACTURING COMPLEX COMPOSITE STRUCTURES WITH FABRIC REINFORCEMENTS.”
- [4] T. Senner, • S Kreissl, • M Merklein, • M Meinhardt, • A Lipp, and M. Merklein, “Bending of unidirectional non-crimp-fabrics: experimental characterization, constitutive modeling and application in finite element simulation,” *Prod. Eng. Res. Devel*, vol. 9, pp. 1–10, 2015.
- [5] J. Cao *et al.*, “Characterization of mechanical behavior of woven fabrics: Experimental methods and benchmark results,” *Compos. Part A Appl. Sci. Manuf.*, vol. 39, no. 6, pp. 1037–1053, Jun. 2008.
- [6] L. Li, Y. Zhao, H. gia nam Vuong, Y. Chen, J. Yang, and Y. Duan, “In-plane shear investigation of biaxial carbon non-crimp fabrics with experimental tests and finite element modeling,” *Mater. Des.*, vol. 63, pp. 757–765, 2014.
- [7] S. Chen, O. P. L. McGregor, L. T. Harper, A. Endruweit, and N. A. Warrior, “Defect formation during preforming of a bi-axial non-crimp fabric with a pillar stitch pattern,” *Compos. Part A Appl. Sci. Manuf.*, vol. 91, pp. 156–167, Dec. 2016.
- [8] G. Creech and A. K. Pickett, “Meso-modelling of Non-Crimp Fabric composites for coupled drape and failure analysis,” *J. Mater. Sci.*, vol. 41, no. 20, pp. 6725–6736, Nov. 2006.
- [9] P. Boisse and P. B. Simulations, *Simulations of Woven Composite Reinforcement Forming*. 2010.
- [10] P. Badel, S. Gauthier, E. Vidal-Sallé, and P. Boisse, “Rate constitutive equations for computational analyses of textile composite reinforcement mechanical behaviour during forming,” *Compos. Part A Appl. Sci. Manuf.*, vol. 40, no. 8, pp. 997–1007, Aug. 2009.
- [11] F. J. Schirmaier, K. A. Weidenmann, L. Kärger, and F. Henning, “Characterisation of the draping behaviour of unidirectional non-crimp fabrics (UD-NCF),” *Compos. Part A Appl. Sci. Manuf.*, vol. 80, pp. 28–38, Jan. 2016.
- [12] P. Harrison, M. J. Clifford, and A. C. Long, “Shear characterisation of viscous woven textile composites: a comparison between picture frame and bias extension experiments,” *Compos. Sci. Technol.*, vol. 64, no. 10–11, pp. 1453–1465, Aug. 2004.
- [13] X. Q. Peng, J. Cao, J. Chen, P. Xue, D. S. Lussier, and L. Liu, “Experimental and numerical analysis on normalization of picture frame tests for composite materials,” *Compos. Sci. Technol.*, vol. 64, no. 1, pp. 11–21, Jan. 2004.